



**HAL**  
open science

## Robustness of cement-based materials: From dosage variations to yield stress fluctuations

Wenqiang Zuo, Hela Bessaies-Bey, Qian Tian, Changwen Miao, Nicolas Roussel

► **To cite this version:**

Wenqiang Zuo, Hela Bessaies-Bey, Qian Tian, Changwen Miao, Nicolas Roussel. Robustness of cement-based materials: From dosage variations to yield stress fluctuations. *Cement and Concrete Research*, 2021, 139, pp.106260 -. 10.1016/j.cemconres.2020.106260 . hal-03493240

**HAL Id: hal-03493240**

**<https://hal.science/hal-03493240>**

Submitted on 9 May 2022

**HAL** is a multi-disciplinary open access archive for the deposit and dissemination of scientific research documents, whether they are published or not. The documents may come from teaching and research institutions in France or abroad, or from public or private research centers.

L'archive ouverte pluridisciplinaire **HAL**, est destinée au dépôt et à la diffusion de documents scientifiques de niveau recherche, publiés ou non, émanant des établissements d'enseignement et de recherche français ou étrangers, des laboratoires publics ou privés.

1 **Robustness of cement-based materials:**  
2 **from dosage variations to yield stress fluctuations**

3  
4 **Wenqiang Zuo<sup>a,b</sup>, Hela Bessaies-Bey<sup>a</sup>, Qian Tian<sup>c,d</sup>, Changwen Miao<sup>b,c,d</sup>, Nicolas**  
5 **Roussel<sup>a\*</sup>**

6  
7 <sup>a</sup> Laboratoire Navier, Université Gustave Eiffel, ENPC, CNRS, F-77447 Marne-la-Vallée,  
8 France

9 <sup>b</sup> School of Materials Science and Engineering, Southeast University, Nanjing 211189,  
10 China

11 <sup>c</sup> Jiangsu Research Institute of Building Science Co.,Ltd, Nanjing 211100, China

12 <sup>d</sup> State Key Laboratory of High Performance Civil Engineering Materials, Nanjing  
13 211100, China

14 \* Corresponding author:

15 Email address: [nicolas.roussel@ifsttar.fr](mailto:nicolas.roussel@ifsttar.fr) (N. Roussel)

16

17 **Abstract**

18 The idea behind the present work is to assess robustness of fresh cement-based  
19 materials (*i.e.* their ability to display the same properties when submitted to  
20 variations in the way they are produced) from a generic and analytical point of view.  
21 First, analytical models from literature relating components proportions and yield  
22 stress are combined into a multi-scale and physical approach and compared to our  
23 experimental yield stress measurements. In the second part, the derivation of these  
24 analytical relationships is used to assess robustness as a function of components  
25 proportions, which allows for the most sensitive variations to be mapped onto  
26 component dosage from a yield stress point of view. In the case of fluid concretes,  
27 this approach showcases the interest of working at slightly higher water content and  
28 slightly lower aggregates fraction along with benefits of viscosity modifying agents /  
29 plasticizers combination.

30

31 **Keywords:** Fresh Concrete (A); Robustness; Yield stress; Rheology (A); Admixture (D)

32        **1. Introduction**

33        In the construction industry, the term “robustness” captures the ability of a product  
34        to display the same properties when submitted to variations in the way it is  
35        processed or used. However, when it comes to concrete, robustness most often  
36        represents the ability of the material to display the same properties when submitted  
37        to either some variations in constituent parts physical and chemical properties or  
38        some variations in constituent parts dosage.

39        In most academic or industrial research laboratories, mix design and sample  
40        production are carried out using only one unique cement batch. Aggregates are  
41        stored in controlled environmental conditions. Dosing and weighting uncertainties  
42        are low compared to industrial practice. For a given mixing process, most  
43        measurements standard deviations are therefore low. Such low standard deviations  
44        allow for the assessment and study of tiny variations in macroscopic properties  
45        typical of today’s research. As a consequence, robustness at the laboratory stage is  
46        often a fully ignored feature of a given mixture.

47        The large volumes of raw material required for industrial concrete production  
48        mandates the use of successive batches of cement and aggregates, increasing the  
49        variation in particle size distribution and fine content. In addition, storage in most  
50        often uncontrolled environmental conditions exacerbates control issues and  
51        variations in aggregate water content in particular. The accuracy in constituent  
52        materials weighing is far lower than in the laboratory. All the above results in higher  
53        variations in constituent parts proportions. In turn, these larger variations in  
54        constituent parts proportions and properties may induce larger variations in the  
55        resulting rheological properties of the fresh material. Consequently, formulations  
56        that had seemed fully adequate in terms of macroscopic properties in the laboratory  
57        may prove difficult to steadily produce on a daily basis at an industrial level. For  
58        instance, Ultra-High Performance Concrete (UHPC) [1] and Self-Compacting Concrete  
59        (SCC) [2] are recent examples of advanced cement-based materials, the commercial  
60        development of which has been hampered by, among others, some robustness

61 issues [3, 4].

62 Robustness of a given cement-based mixture is however an extremely delicate  
63 feature to tackle, as it often requires numerous experiments in order to capture  
64 variations in macroscopic behavior induced by variations in constituent parts  
65 properties and dosages. The most sensitive (or most critical) constituent properties  
66 or proportions may vary from one mix design to another. For instance, low W/C ratio  
67 concretes are far more sensitive to water content variations than high W/C ratio  
68 mixes whereas low slump concretes can be more sensitive to sand/gravel ratio than  
69 standard flowable concretes.

70 The idea behind the present work is therefore to make use of the most recent  
71 analytical models from literature allowing for the prediction of fresh properties of  
72 cement-based materials as a function of constituent parts properties and  
73 proportions. The obvious advantage of such relationships lies in their analytical  
74 nature, which offers the possibility to derive them and assess robustness from a  
75 generic and analytical point of view. This, in turn, may allow for a reduction of the  
76 amount of experimental measurements required to assess the robustness of a given  
77 cement based-mixture.

78 This above generic idea is illustrated in this work by a fluid concrete example (*i.e.*  
79 slump flow higher than 50 cm) although the same work could be carried out for  
80 other types of cement-based materials. The approach and the analytical relations  
81 used here would be the exact same ones. In this study, it is assumed that all  
82 components properties are fixed. The variations, to which the material is submitted,  
83 are only, therefore, the respective proportions of its constituent parts. This would  
84 correspond in practice to a situation, in which the material is produced from the  
85 same batches of constituents. Moreover, in this study, the focus is limited to the yield  
86 stress of the resulting mixture and its variations, as this rheological parameter is the  
87 most documented in literature and the most important in standard casting processes  
88 [5].

89 The objective of the first part of this paper is therefore to show how component  
90 proportions variations affect yield stress from the polymer adsorption scale to the

91 concrete scale. Analytical models from literature relating components proportions  
92 and yield stress are combined into a multi-scale and physical approach and compared  
93 to our experimental yield stress measurements.

94 In the second part of this paper, from the derivation of these analytical relations, we  
95 assess robustness as a function of components proportions and map the most  
96 sensitive variations in components dosage from a yield stress point of view.

97 Finally, in the specific case of the fluid concrete taken here as an example, we  
98 conclude on the potential changes in mix design that may result into a more robust  
99 mixture.

100

## 2. Background and methodology

First, it is important to make a distinction between material parameters that capture the constituent parts properties and are therefore non-dependent on mix proportions and the mixture variables, which result directly from mix proportions.

In this section, from literature, the number and nature of the variables theoretically required to describe one cubic meter are derived in the case of an optimized fluid concrete with a given yield stress and containing five constituents: water, cement, sand, gravel and a super-plasticizer (SP). The proportion of each of these five constituents is obviously a mixture variable by itself. However, when dealing with the proportions required to produce one cubic meter of concrete, it is therefore possible to describe all components proportions with only four mixture variables. Additionally, as the yield stress of the concrete is specified, this provides an additional relation, which leads to reduce the number of independent mixture variables to three. Finally, it is considered in this study that the studied mix has already been optimized. As a consequence, the aggregates size distribution and the relative proportion between sand and gravel have both already been fixed in order to maximize the packing properties (*i.e.* the maximal packing fraction) of the granular skeleton [6-8]. Such a material should therefore be fully described by using only two independent mixture variables. A mineral filler would often be added to such a mixture in order to reduce carbon foot print, to improve workability and to decrease cost, shrinkage and hydration heat according to [9-11] and ASTM C 1797. This would, in turn, increase the number of variables required to describe the mixture to three. For the sake of simplicity, this situation is however out of the scope of the present paper.

In order to identify and select the two previous variables, the present approach is based on several analytical relations from literature, which have all proved, in previous publications from various authors, their ability to predict the related underlying physics. These analytical relations include:

### 2.1. YODEL model for cement pastes

130 The Yodel is a first principle analysis of yield stress of colloidal particles suspension. It  
 131 was shown to successfully predict the main parametric dependencies of cement  
 132 suspensions yield stress [12-15]. This model is used here to predict the yield stress  
 133  $\tau_p$  of the constitutive cement paste of the concrete (*i.e.* the matrix phase). The  
 134 model can be written as:

$$\tau_p \cong m \frac{A_0 a^* \varphi_c^2 (\varphi_c - \varphi_{perc})}{d^2 H^2 \varphi_{cm} (\varphi_{cm} - \varphi_c)} \quad (1)$$

135 Where 6 material parameters are:

136 *m*, a pre-factor, which depends on the cement particle size distribution; It  
 137 is possible to compute it from the cement particle size distribution but it is  
 138 simpler to measure the value of the product  $m A_0 a^*$  in Eq. (1) on a  
 139 reference cement paste as shown in [14, 15].

140  $A_0$ , the non-retarded Hamaker constant taken as  $1.6 \times 10^{-20}$  J [12];

141  $a^*$ , the typical size of the surface defects of cement grains of the order of  
 142 several hundreds of nm [15];

143  $d$ , the cement particle volume-average diameter  $d_{50}$  of the order of 10  
 144  $\mu\text{m}$ . It can be measured using laser granulometry (see next section);

145  $\varphi_{cm}$ , the maximal packing fraction of the cement powder. It can be  
 146 measured using the water demand method developed by De Larrard (see  
 147 next section) [6].

148  $\varphi_{perc}$ , the percolation volume fraction; It results from the competition  
 149 between Brownian motion and colloidal attractive forces between cement  
 150 particles, which, in turn, depend on the SP dosage [15]. This dependency is  
 151 however weak. It is therefore considered here as a constant material  
 152 parameter. It can be extrapolated from a yield stress measurement on a  
 153 reference cement paste as described in [14, 15].

154 And where 3 mixture variables are:

155  $\tau_p$ , the yield stress of the constitutive cement paste of the concrete;

156  $\varphi_c$ , the solid volume fraction of cement particles in the cement paste;

157  $H$ , the average surface-to-surface separating distance between



158 *flocculated cement particles; It depends on the SP dosage as described in*  
159 *sub-section 2.2.*

160

## 161 **2.2. Statistical average separating distance between cement grains as a function** 162 **of admixture surface coverage**

163 The average separating distance between cement grains  $H$  [14] can be computed as:

$$\frac{1}{H^2} = \frac{\theta^2}{H_p^2} + \frac{8\theta(1-\theta)}{(H_p + H_0)^2} + \frac{(1-\theta)^2}{H_0^2} \quad (2)$$

164 *Where 2 additional material parameters are:*

165  *$H_p$ , the SP layer thickness at full surface coverage. It could be estimated from*  
166 *the molecular structure of the SP [16]. It is however easier in practice and*  
167 *when faced with an unknown molecular structure to assess its value from*  
168 *yield stress measurements on fresh cements pastes containing a given*  
169 *dosage of SP [15];*

170  *$H_0$ , the average separating distance between cement grains in a system not*  
171 *containing any admixtures (of the order of 1-2 nm) [17].*

172 *And where 1 mixture parameter is:*

173  *$\theta$ , the so-called “surface coverage” or the ratio between the amount of SP*  
174 *adsorbed and the amount of adsorbed SP at surface saturation, which can*  
175 *be extracted from an adsorption isotherm (see below).*

176

## 177 **2.3. Surface coverage as function of SP dosage**

178 It is now accepted that any mathematical relations showing a proportionality at low  
179 dosages between SP dosage and SP adsorption and displaying an adsorption plateau  
180 at high SP dosages is able to capture the adsorption behavior of a given SP and the  
181 surface coverage evolution as function of SP dosage [18, 19]. Langmuir-type relation  
182 is an example of this kind of mathematical relations. In this work, for the sake of  
183 simplicity, the following analytical relation is used:

$$\theta = \frac{\kappa \cdot D_{rsp}}{1 + \kappa D_{rsp}} \quad (3)$$

184 Where  $D_{rsp}$  is an additional mixture parameter, defined as the relative dosage of SP  
 185 with  $D_{rsp} = D_{sp}/D_{sat}$ , where  $D_{sp}$  is the SP dosage expressed as a mass  
 186 proportion of the cement content per cubic meter and  $D_{sat}$  is the so-called  
 187 saturation dosage (see below);

188 And where 2 material parameters are:

189  $\kappa$ , a dimensionless adsorption and desorption equilibrium rate constant;  $\kappa$   
 190 can be assessed from the measurement of the polymer adsorption isotherm;  
 191  $D_{sat}$ , the so-called saturation dosage, above which further increase in the  
 192 dosage of SP does not increase the surface coverage. It can be assessed  
 193 through SP adsorption measurements or yield stress measurements.

194

#### 195 **2.4. Chateau and Ovarlez model for mortar and concrete yield stress**

196 The Chateau and Ovarlez model has proven its ability to predict the yield stress of a  
 197 mixture containing rigid inclusions in a yield stress fluid [20, 21]. It was moreover  
 198 shown to be able to predict the yield stress of fluid mortars and concretes when  
 199 direct frictional contacts between aggregates were neglectable (*i.e.* high matrix  
 200 volume content and/or fluid mixtures [7]). It can be expressed as:

$$\tau_M = \tau_p \sqrt{(1 - \varphi)} \left(1 - \frac{\varphi}{\varphi_{div}}\right)^{-1} = \tau_p \sqrt{(1 - \varphi)} \left(1 - \frac{\varphi}{0.8\varphi_{am}}\right)^{-1} \quad (4)$$

201 Where 2 additional mixture parameters are:

202  $\tau_M$ , the yield stress of the mortar or concrete mixture;  
 203  $\varphi$ , the aggregates volume fraction at the level of one cubic meter of  
 204 concrete;

205 And where one material parameter is:

206  $\varphi_{div}$ , the aggregates volume fraction for which the yield stress diverges. It  
 207 was shown that, for sand, gravels and fibers,  $\varphi_{div} = 0.80\varphi_{am}$ , where  $\varphi_{am}$   
 208 is the maximal packing fraction of the aggregates [7, 22].  $\varphi_{am}$  can be  
 209 measured using independent compaction measurements carried on the dry

210 aggregates [23].

211

## 212 **2.5. Integration of all models**

213

214 The yield stress  $\tau_M$  of a fluid concrete can therefore, in theory, be predicted  
215 combining equations ((1) to (4)). Such an approach would involve the 11 material  
216 parameters listed above that do capture both the components properties and their  
217 interactions. These 11 parameters can all be experimentally and independently  
218 assessed. Because of the way the above analytical relations are built, these  
219 parameters are only component-dependent and not dosage-dependent (*i.e.* they do  
220 not change when varying components proportions).

221 The full description of the mixture from the above equations moreover involves  
222 seven mixture variables along with four multi-scale relations. This results into 3  
223 independent variables. For these variables, the cement solid volume fraction  $\varphi_c$  at  
224 the scale of one cubic meter of the constitutive cementitious matrix (*i.e.* excluding  
225 any aggregates), the SP dosage  $D_{sp}$  (*i.e.* the mass ratio between SP and cement) and  
226 the aggregates volume fraction  $\varphi$  at the scale of one cubic meter of concrete or  
227 mortar were selected. As stated previously, only two of these three variables are  
228 enough to describe such a system if a target value for its yield stress is first specified.

229

## 230 **3. Materials and experimental protocols**

231

### 232 **3.1. Materials properties**

233 A commercial cement equivalent to ASTM Type I cement was used in this study. The  
234 chemical composition of the cement is shown in Table 1. The Particle Size  
235 Distribution (PSD) was measured by laser diffraction (MALVERN MASTERSIZER S)  
236 after dispersion in isopropanol and its volume average diameter  $d_{50}$  was around 12  
237 micrometers (Cf. **Fig. 1**). The maximum packing fraction of this cement was 0.58. It  
238 was measured following the water demand method developed by De Larrard [6]. It

239 consists in finding the minimum water content allowing for the transition during  
240 mixing between pasty cement granules and a continuous homogeneous paste.

241

242 The properties of the aggregates used in this study are shown in **Table 2** and the PSD  
243 of the aggregates is shown in Fig. 1. The maximal packing fraction of the aggregates  
244 was measured using the following protocol. A container with the diameter and  
245 height of 16 cm and 32 cm respectively was fixed on a vibration table and was  
246 submitted to a 150 Hz vibration. A mass, equivalent to 1 kPa external pressure, was  
247 applied above the sample. For each dry batch of aggregates, 7.5 kg of aggregates  
248 were poured into the container and, after a 60 s vibration, the height of the sample  
249 was measured. Finally, using the mean apparent density of the aggregate mixtures,  
250 the maximum packing fraction was computed.

251 In addition to the independent assessment of sand and gravel, the packing properties  
252 of dry mixtures of sand and gravel with varying proportions were also measured (Cf.  
253 **Fig. 2**). The sand mass proportion was then chosen in order to optimize the packing  
254 properties of the granular skeleton and is therefore equal to 45%.

255 The SP used in this study is a non-blended commercial polycarboxylate provided  
256 under liquid form with a solid content of 29.5%. The recommended highest dosage of  
257 this SP is 3.0% by mass of cement.

258

### 259 **3.2. Mixing protocols**

260 Cement pastes with different dosages of SP ranging from 0% to 3.5% were prepared.  
261 The SP was first added into the mixing water (with controlled temperature of around  
262  $22 \pm 2^\circ\text{C}$ ) prior to the contact with cement. For each dosage of SP, cement pastes  
263 with  
264 W/C mass ratio ranging from 0.275 to 0.5 were prepared. For each sample, a volume  
265 of around 200 ml of cement paste was mixed for 3 min using a Turbo test Rayneri  
266 VMI mixer at the speed of 840 rpm. A total of 53 different cement pastes was  
267 prepared.

268 The mortars were produced from cement pastes prepared using the same protocol  
269 as above. Then, the sand was introduced into the cement paste and stirred for 2 min  
270 by hand in order to decrease the influence of mixing in the presence of rigid particles  
271 on the rheological properties of the interstitial constitutive cement paste [14]. The  
272 sand content was varied from 0 to 52.5% volume fraction (*i.e.* around 475 liters of  
273 paste per cubic meter) while the W/C ratio and SP mass dosage were varied between  
274 0.275 to 0.50 and between 0 and 3% respectively in order to produce 41 different  
275 mortars.

276 In the case of concrete mixing, a Zyklos-type concrete mixer from Schwelm was used.  
277 The corresponding cement paste was first mixed alone for 3 min then the aggregates  
278 were introduced and dispersed for another 2 min. We checked that the cement  
279 pastes prepared in this mixer had a similar yield stress as the ones prepared with the  
280 Rayneri mixer above (results not shown here). Around 10 liters of concrete were  
281 produced for each concrete mixture. The total aggregate content was varied from  
282 zero to around 62% volume fraction (*i.e.* around 380 liters of paste per cubic meter of  
283 concrete) over 5 different concretes mixes.

284 All experiments were carried out at a temperature of  $22 \pm 2^\circ\text{C}$  and at a relative  
285 humidity of around  $50\% \pm 5\%$ .

286 All mix designs are provided as supplementary materials along with measured yield  
287 stress values.

288

### 289 **3.3. Yield stress measurements**

290 In this study, the values of the yield stress of cement pastes, mortars and concrete  
291 mixtures were computed from simple flow tests [7, 24].

292 At the scale of cement paste and mortar, volumes of around 200 ml and around 500  
293 ml were used respectively to measure flow spread. Each mixture was slowly poured  
294 from the mixing cup on a horizontal steel plate. The spread diameter was assessed  
295 from the average of two measured diameters. The yield stress value was then  
296 computed using the following equation [24, 25]:

$$\tau_0 = \frac{225\rho g\Omega^2}{128\pi^2 R^5} \quad (5)$$

297 where  $\tau_0$  is the yield stress (Pa);  $\rho$  is the bulk density of the mixture ( $\text{kg/m}^3$ );  $\Omega$  is  
 298 the volume of the mixture ( $\text{m}^3$ );  $R$  is the spread radius (m).

299 At the scale of concrete, 6 l of material were slowly poured from a bucket into one  
 300 end of the LCPC box and the spread length was measured [26]. The yield stress of the  
 301 concrete mixtures was computed from the existing analytical correlation between  
 302 the measured spread length in the LCPC box and the yield stress of the tested  
 303 material [26, 27] (Cf. Eq. (6) and (7)).

$$V = \frac{l_0^3}{4A} [LN(1 + U_0)] + \frac{U_0(U_0 - 2)}{2} \quad (6)$$

$$L = \frac{h_0}{A} + \frac{l_0}{2A} LN\left(\frac{l_0}{l_0 + 2h_0}\right) \quad (7)$$

304 where  $V$  is the tested concrete volume (L);  $l_0$  the width of the LCPC box (20 cm);  $L$   
 305 the measured spread length of concrete in the box (cm);  $h_0$  the height of the  
 306 sample at the point where concrete is poured at the end of the test (cm);  $A =$   
 307  $2\tau_0/\rho g l_0$ ,  $U_0 = 2h_0/l_0$ , where  $\tau_0$  is the yield stress of the concrete (Pa),  $\rho$  the  
 308 apparent density of the concrete ( $\text{kg}\cdot\text{m}^{-3}$ ),  $g$  the gravity ( $\text{m}\cdot\text{s}^{-2}$ ). Solving the above  
 309 equations simultaneously provides the value of the concrete yield stress. An abacus  
 310 is also available in [26].

311

### 312 **3.4. Polymer adsorption measurements**

313

314 A total organic carbon (TOC) analyzer manufactured by Shimadzu was used in this  
 315 work. Cement pastes with W/C equal to 0.4 and dosages of SP ranging from 0 % to  
 316 3.5% by mass of cement were mixed as described above. The cement pastes were  
 317 then centrifuged and the extracted interstitial fluid was diluted and analyzed. By  
 318 comparing the TOC values of the extracted interstitial fluid with a reference polymer  
 319 solution, the amount of polymer adsorbed on cement grains was computed and the  
 320 surface coverage (*i.e.* the ratio between adsorbed polymer and adsorbed polymer at  
 321 saturation) as a function of the polymer relative dosage (*i.e.* ratio between dosage

322 and saturation dosage) is plotted in **Fig. 3**. The amount of organic carbon in the  
323 interstitial fluid of a reference cement paste without polymer was also measured to  
324 account for the presence in the cement powder of organic compounds such as  
325 grinding agents.

326

## 327 **4. Experimental results and analysis of results**

### 328 **4.1. Yield stress of cement paste**

329 The yield stress of cement paste as a function of cement volume fraction for various  
330 SP dosages is plotted in **Fig. 4**. Only non-bleeding cement pastes (visual observation)  
331 are shown in **Fig. 4**. The values of the measured yield stress range from around 1 Pa  
332 to around 100 Pa. It should be noted that the higher the SP dosage, the higher the  
333 minimum cement volume fraction required to obtain a non-bleeding mixture.

334 The prediction of the yodel model is also plotted in **Fig. 4** (continuous lines). It is  
335 worth noting that the only parameter changing from one SP dosage to another in the  
336 Yodel is the average surface-to-surface separation distance ( $H$ ) between cement  
337 particles (not shown here). This distance is varied from 2 nm (reference paste) to 9  
338 nm (full surface coverage). As already shown in previous papers [12, 13], the YODEL  
339 analytical model is able to capture the evolutions of a cement paste yield stress as a  
340 function of solid volume fraction and inter-particle distance over more than two  
341 orders of magnitude.

342

### 343 **4.2. Yield stress of mortar**

344 **Fig. 5** shows the relative yield stress of the tested mortars (*i.e.* the ratio between the  
345 mortar yield stress and the yield stress of the corresponding constitutive cement  
346 paste) as a function of sand volume fraction for sand volume fractions varying from 0%  
347 to around 50%. It can be seen that the values of the relative yield stress range from 1  
348 to around 50 times the yield stress of the corresponding constitutive cement pastes.  
349 Interestingly but as already shown in [23] and as predicted by the Chateau and  
350 Ovarlez model, the relative yield stresses of the studied mortars does not depend on

351 the yield stress of the constitutive cement pastes. The amplification of the  
352 constitutive paste behavior by the rigid sand particles is well predicted in **Fig. 5** by  
353 the Chateau and Orvarlez model without any need for fitting nor corrections.

354 As predicted by Eq. (4), when the relative solid volume fraction (*i.e.* the ratio  
355 between the sand volume fraction and the maximum packing fraction of the sand as  
356 measured in section 3.1) approaches  $0.80\varphi_{am}$  (dotted vertical line in **Fig. 5**), the  
357 yield stress of the tested mortars shows a sharp increase of a couple orders of  
358 magnitude [7, 22]. This feature indicates that frictional contacts between sand grains  
359 start to percolate and dominate the macroscopic rheology of the mixtures [20, 21,  
360 23].

361

### 362 **4.3. Yield stress of concrete**

363 **Fig. 6** represents the relative yield stress of the concrete (*i.e.* the ratio between the  
364 yield stress of the concrete and the yield stress of the constitutive cement paste) as a  
365 function of the total aggregate volume fraction (*i.e.* sand and gravel). The relative  
366 yield stress predicted by the Chateau and Ovarlez model is also plotted in **Fig. 6**. As  
367 expected from the previous section, the model captures the experimental data and  
368 shows a divergence as the aggregates volume fraction reaches the divergence  
369 volume fraction around 62% (vertical dotted line in **Fig. 6**).

370

## 371 **5. Robustness assessment**

### 372 **5.1. Robustness index definition**

373 In order to assess the robustness of a given mixture, we define here a robustness  
374 index  $R_\tau$  for a component dosage variation. As yield stress is the parameter of  
375 interest in this study, such an index can be expressed as follows:

$$R_\tau = \frac{d\tau_m}{dx} \cdot \frac{\Delta x_{max}}{\tau_m} \quad (8)$$

376 where  $R_\tau$  is the robustness index from the yield stress point of view (dimensionless).  
377  $\tau_m$  is the yield stress of the mixture (Pa);  $x$  stands for the dosage of one of the  
378 mixture components while  $\Delta x_{max}$  is the maximum variation of this dosage in



379 industrial practice. In order to define  $\Delta x_{max}$ , the average variations of components  
380 dosage in concrete plants from various technical recommendations and studies [28,  
381 29] are considered (Cf. **Table 3**). It has to be noted that the derivation in Eq. (8)  
382 includes the fact that, if the volume of one component is increasing or decreasing,  
383 then the volume of all other components has to be decreased or increased  
384 respectively in order to cover for the total volume change at the level of the  
385 considered one cubic meter of concrete. This effect is neglectable for SP and cement  
386 dosage variations but plays a non-neglectable role for aggregates and water dosages  
387 variations. Finally, it has to be kept in mind that, in the following, the higher the  
388 robustness index, the less robust is the mix.

389 It can first be noted that the more restrictive values from the ACI standards [28]  
390 seem to be closer to real industrial practice when compared to the  
391 industry-representative values reported in literature [30-32]. We choose therefore to  
392 consider these limits in this study.

393 However, the water dispenser accuracy from the ACI standard [28] in **Table 3** does  
394 not take into account some potential uncertainties on the moisture content of the  
395 sand [4, 33]. These are reported to be measured with a 0.5% accuracy for most  
396 existing sensors as reported in technical data sheets for this kind of sensors. Some  
397 more accurate water-moisture online assessment technologies do exist but we do  
398 not consider that they are representative of the common practice.

399 Moreover, we choose here to turn these relative uncertainties requirement for  
400 standard concrete production into absolute uncertainties in order to extrapolate the  
401 consequences on robustness of these variations for non-standard component  
402 dosages. In order to do so, we consider that the previous uncertainties are given for  
403 one cubic meter of standard concrete that is considered here to contain 300 kg of  
404 cement, 150 kg of water, 800 kg of sand, 1200 kg of gravel and 3 kg of  
405 super-plasticizer. The absolute variation for water dosage is then computed as the  
406 square root of the sum of the water dispenser accuracy (4.5 kg) at the power two  
407 and the uncertainty of the sand moisture sensor (4 kg) at the power two resulting in  
408 an overall absolute uncertainty of 6 kg. Due to the fact that the accuracy of adding SP

409 might be difficult to guarantee during the opening and closing of the SP feed port, a  
410 higher absolute variation for SP dosage (i.e. 150 g) is considered according to the EHE  
411 limits [29].

412 Finally, we choose here to ignore any potential variations in the sand-to-gravel ratio  
413 and only consider variations in the total aggregate content. The reason behind is that  
414 aggregates influence on yield stress is mostly driven by total solid fraction and  
415 maximum packing fraction of the sand-gravel mixture. However, variations in sand to  
416 gravel ratio for an optimized mixture of aggregates do not induce strong variations in  
417 maximum packing fraction. Indeed, around the optimal sand-gravel proportions,  
418 variations in maximum packing properties of the resulting granular skeleton are  
419 neglectable as illustrated in this work in **Fig. 2**. Similar to water dosage variations, the  
420 overall absolute uncertainty on the total aggregate content is then computed from  
421 the combined variations in sand and gravel content and reported in **Table 3**.

422

## 423 **5.2. Robustness maps**

### 424 **5.2.1. SP dosage variations**

425 **Fig. 7** represents the robustness index for SP dosage variations. It is plotted for the  
426 150g SP dosage variation from **Table 3** for W/C between 0.3 and 0.55 and relative  
427 aggregates content (i.e. the ratio between aggregates volume fraction and maximum  
428 packing fraction) between 74 and 79%. This W/C range is typical of most fluid  
429 concretes as it covers high strength materials (excluding ultra-high-performance  
430 material) for civil engineering application along with standard concretes for housing  
431 applications. Obviously, lower W/C shall lead to better mechanical and transfer  
432 properties while higher aggregates volume fraction shall result in cheaper mixes as  
433 they lead to lower matrix and cement content. Two features bound the range  
434 covered here by the aggregates relative fraction variation. On one hand, for the  
435 highest aggregates relative fraction, as illustrated in **Fig. 6**, it is not possible to mix  
436 design a stable fluid material as direct frictional contacts between aggregates  
437 dominate [7]. No matter the amount of water or SP, the material shall either display a  
438 high yield stress or be unstable [34]. On the other hand, for lowest aggregates

439 relative fraction, the matrix volume becomes high inducing potential shrinkage,  
440 hydration heat and/or creep issues [35].

441 For a SP saturation dosage taken as 2% of the cement mass, **Fig. 7** shows that the  
442 highest robustness index is around 20% (*i.e.* 10 Pa variation) and occurs for the  
443 highest W/C and lowest relative aggregates volume fraction. It is indeed in this mix  
444 design range that the dosage of SP is the lowest. As a consequence, the relative  
445 variation in SP dosage for a given dosage accuracy is the highest. This feature is  
446 amplified by the shape of the adsorption isotherm in **Fig. 3**. Indeed, as the dosage of  
447 SP gets closer to the saturation dosage, the sensitivity of surface coverage to SP  
448 dosage decreases and the system becomes more robust from a SP dosage point of  
449 view. This is one of the reasons why admixtures manufacturers often recommend a  
450 minimum SP dosage. This minimum dosage ensures that the resulting mix is not too  
451 sensitive to SP dosage variation in industrial production. As a consequence, at high  
452 W/C, it is obviously safer to use a less efficient SP that would require a higher dosage  
453 to get a similar yield stress. For instance, the robustness index values around 20% in  
454 **Fig. 7** become of the order of 15% if the saturation dosage of the SP used increases  
455 from 2% to 3% (*i.e.* less effective SP).

456

### 457 **5.2.2. Cement dosage variations**

458 **Fig. 8** represents the robustness index for cement dosage variations. It is plotted for  
459 the 3 kg cement dosage accuracy from **Table 3**. Firstly, it can be noted that the  
460 mixture is far less sensitive to standard cement variations than it is to standard SP  
461 variations. Moreover, it can be noted that the trend here is more complex with  
462 different regimes clearly appearing, namely for low and high W/C and for high  
463 relative aggregates volume fractions.

464 It is first obvious that the system is more sensitive to cement dosage variation when  
465 the W/C is low. Indeed, at high cement volume fractions (*i.e.* close to the cement  
466 powder maximum packing fraction), as shown in **Fig. 4**, despite the log scale, yield  
467 stress shows an extremely high sensitivity to solid volume fraction.

468 At high W/C, on the other hand, the dosage of SP and the resulting surface coverage

469 is low. A variation in cement content result therefore in a variation in surface  
470 coverage, which, in turn, induces variations in yield stress as discussed above for **Fig.**  
471 **7**.

472 Finally, at high relative aggregates volume fractions, our analysis suggests that the  
473 higher sensitivity of the mixture finds its origin in the fact that, at the level of one  
474 cubic meter, a decrease in cement dosage results in a relative increase in aggregates  
475 content. Such systems are however close to the divergence aggregates volume  
476 fraction illustrated in **Fig. 6** and are therefore very sensitive to small fluctuations in  
477 aggregate content.

478 Overall, however, it will be seen further that fluctuations in yield stress induced by  
479 cement dosage variations are neglectable compared to the other sources of  
480 fluctuations.

481

### 482 **5.2.3. Water dosage variations**

483 **Fig. 9** represents the robustness index for water dosage variations. It is plotted for  
484 the 6 kg water dosage accuracy from **Table 3**. The high sensitivity of the system to  
485 water dosage compared to SP and cement can first be noted. Moreover, as W/C is  
486 decreasing, the sensitivity of the mixture to water variations increases. This finds its  
487 origin in the robustness of the cement paste itself that decreases at low W/C as  
488 shown in **Fig. 4** where the yield stress, for high solid fractions, shows an extremely  
489 high sensitivity to solid volume fraction.

490 We moreover note that, when the relative aggregate volume fraction increases, the  
491 sensitivity of the mixture to water increases. This unexpected trend finds its origin in  
492 the indirect consequence of a decrease in water dosage at the scale of one cubic  
493 meter. If the water content decreases, the proportions of all other components  
494 increase. A 6 liters variation in water is indeed able to induce a 15 kg variation in  
495 aggregate content or around 20 kg in cement dosage. As shown previously, cement  
496 content variations only had minor consequences. This is not the case for aggregates  
497 content, especially at high aggregate fractions when yield stress becomes extremely  
498 sensitive to aggregate content as shown in **Fig. 6**.

499

#### 500 **5.2.4. Aggregate dosage variations**

501 **Fig. 10** shows the robustness index for aggregate dosage variations. It is plotted for  
502 the 29 kg total aggregate dosage accuracy from **Table 3**. Firstly, it can be noted that  
503 this graph shows the second highest sensitivity after water variations (Cf. **Fig. 10**).  
504 The robustness index does not depend on the W/C ratio but only on the relative  
505 aggregates solid volume fraction. For high aggregate fractions, yield stress becomes  
506 extremely sensitive to aggregate content as shown in **Fig. 6**.

507

#### 508 **5.2.5. Practical consequences on the mix design of robust fluid concretes**

509 **Fig. 11** shows the overall sensitivity map of the fluid concrete taken as an example  
510 here by computing the quadratic average of all the above robustness indexes.  
511 Unsurprisingly, the overall answer is dominated by the influence of water variations  
512 and aggregates dosage variations. As a consequence, although the most economical  
513 mixtures shall be obtained for aggregates relative solid fraction close to 80%, **Fig. 11**  
514 suggests that mixtures with acceptable robustness are obtained for lower aggregates  
515 dosages than the economical optimum.

516 Moreover, **Fig. 11** suggest that more robust mix could be produced by moving to  
517 higher W/C ratio (when obviously mechanical strength and durability are not an  
518 issue). This could reach a limit at high W/C ratio combined with lower aggregates  
519 dosage as it would lead to a decrease in the SP dosage required and bring the system  
520 to the darkest zone of Fig. 7 where the mixture becomes very sensitive to SP dosage.  
521 One solution would then be to combine the SP with a viscosity modifying agent  
522 (VMA). The resulting adsorption competition between these molecules [36, 37]  
523 would increase the required SP dosage and decrease therefore the sensitivity of the  
524 mixture to SP dosage. It should be noted that this solution seems to be adopted in  
525 many countries where Self-compacting Concretes are designed with VMAs. Our  
526 results suggest, however, that VMAs do not increase robustness directly as  
527 sometimes suggested [38] but, instead, allow for the design of mixtures with higher  
528 water content or higher SP dosages, which are, in turn, more robust.

529 Finally, as both aggregates content and water dosage are strongly correlated to  
530 aggregates water content and aggregates water content measurement, it can be  
531 extrapolated that, from a concrete production point of view, it is on its ability to  
532 measure aggregates water content that the concrete plant technology performance  
533 has the strongest influence on a fluid concrete robustness.

534

## 535 **5 Conclusions**

536 The idea behind the present work was to assess robustness of fresh cement-based  
537 materials from a generic and analytical point of view.

538 In a first part, analytical models from literature relating components proportions and  
539 yield stress were combined into a multi-scale and physical approach and compared  
540 to our experimental yield stress measurements.

541 In the second part of this paper, from the derivation of these analytical relations, we  
542 assessed robustness as a function of constituent parts proportions and mapped the  
543 most sensitive variations in constituent parts proportions from a yield stress point of  
544 view.

545 The results in this investigation demonstrated the dominant sensitivity of the mixture  
546 to water and aggregates dosages and, indirectly, to aggregates moisture variations.  
547 Although these results are known in practice, the work presented here allows, for the  
548 first time, for the quantitative prediction of concrete robustness.

549 Moreover, the results, obtained here in the case of the fluid concrete taken as an  
550 example of the methodology, provide some physical explanations for the positive  
551 effect on robustness of some trends in SCC mix design. For instance, working with  
552 slightly lower fractions of aggregates than the economical *optimum* brings the  
553 system further from the aggregates contact percolation packing fraction where the  
554 sensitivity of the system to aggregates dosage is the highest. Similarly, increasing  
555 slightly the water content brings the system further from the cement powder  
556 maximum packing fraction where the sensitivity to water dosage is the highest.  
557 However, increasing water dosage and decreasing aggregate content both induce a

558 decrease in the required plasticizer dosage. This, in turn, increases the sensitivity of  
559 the mixture to plasticizer dosage. Combining viscosity modifying admixtures with  
560 plasticizers, because of their competitive adsorption, is a potential way to go back to  
561 standard plasticizer dosages and improve robustness.

562

### 563 **Acknowledgement**

564 The authors would like to acknowledge the financial support from National Natural  
565 Science Foundation of China (No. 51890904, No. 51708108).

566

### 567 **Conflict of interest**

568 The authors declare that they have no conflict of interest.

569

### 570 **Reference**

- 571 [1] B.A. Graybeal, Material property characterization of ultra-high performance concrete, in, United  
572 States. Federal Highway Administration. Office of Infrastructure ..., 2006.
- 573 [2] H.J.H. Brouwers, H.J. Radix, Self-Compacting Concrete: Theoretical and experimental study, *Cement*  
574 *and Concrete Research*, 35 (2005) 2116-2136.
- 575 [3] I. González-Taboada, B. González-Fonteboa, F. Martínez-Abella, N. Roussel, Robustness of  
576 self-compacting recycled concrete: analysis of sensitivity parameters, *Materials and Structures*, 51  
577 (2018) 8.
- 578 [4] S. Naji, S.-D. Hwang, K.H. Khayat, Robustness of self-consolidating concrete incorporating different  
579 viscosity-enhancing admixtures, *ACI materials journal*, 108 (2011) 432.
- 580 [5] N. Roussel, Rheology of fresh concrete: from measurements to predictions of casting processes,  
581 *Materials and Structures*, 40 (2007) 1001-1012.
- 582 [6] F. De Larrard, *Concrete mixture proportioning: a scientific approach*, CRC Press, 2014.
- 583 [7] J. Yammine, M. Chaouche, M. Guerin, M. Moranville, N. Roussel, From ordinary rheology concrete  
584 to self compacting concrete: A transition between frictional and hydrodynamic interactions, *Cement*  
585 *and Concrete Research*, 38 (2008) 890-896.
- 586 [8] F. De Larrard, T. Sedran, Mixture-proportioning of high-performance concrete, *Cement and*  
587 *concrete research*, 32 (2002) 1699-1704.
- 588 [9] F.V. Mueller, O.H. Wallevik, K.H. Khayat, Linking solid particle packing of Eco-SCC to material  
589 performance, *Cement and Concrete Composites*, 54 (2014) 117-125.
- 590 [10] W. Zuo, W. She, W. Li, P. Wang, Q. Tian, W. Xu, Effects of fineness and substitution ratio of  
591 limestone powder on yield stress of cement suspensions, *Materials and Structures*, 52 (2019) 74.
- 592 [11] G. Ye, X. Liu, G. De Schutter, A.-M. Poppe, L. Taerwe, Influence of limestone powder used as filler  
593 in SCC on hydration and microstructure of cement pastes, *Cement and Concrete Composites*, 29 (2007)

594 94-102.

595 [12] R.J. Flatt, P. Bowen, Yodel: a yield stress model for suspensions, *Journal of the American Ceramic*  
596 *Society*, 89 (2006) 1244-1256.

597 [13] R.J. Flatt, P. Bowen, Yield stress of multimodal powder suspensions: an extension of the YODEL  
598 (Yield Stress mODEL), *Journal of the American Ceramic Society*, 90 (2007) 1038-1044.

599 [14] J. Hot, H. Bessaies-Bey, C. Brumaud, M. Duc, C. Castella, N. Roussel, Adsorbing polymers and  
600 viscosity of cement pastes, *Cement and concrete research*, 63 (2014) 12-19.

601 [15] A. Perrot, T. Lecompte, H. Khelifi, C. Brumaud, J. Hot, N. Roussel, Yield stress and bleeding of fresh  
602 cement pastes, *Cement and Concrete Research*, 42 (2012) 937-944.

603 [16] R. Flatt, I. Schober, Superplasticizers and the rheology of concrete, in: *Understanding the*  
604 *rheology of concrete*, Elsevier, 2012, pp. 144-208.

605 [17] G. Gelardi, R. Flatt, Working mechanisms of water reducers and superplasticizers, in: *Science*  
606 *and Technology of Concrete Admixtures*, Elsevier, 2016, pp. 257-278.

607 [18] D. Marchon, S. Mantellato, A. Eberhardt, R. Flatt, Adsorption of chemical admixtures, in:  
608 *Science and Technology of Concrete Admixtures*, Elsevier, 2016, pp. 219-256.

609 [19] R.J. Flatt, I. Schober, E. Raphael, C. Plassard, E. Lesniewska, Conformation of adsorbed comb  
610 copolymer dispersants, *Langmuir*, 25 (2008) 845-855.

611 [20] X. Chateau, G. Ovarlez, K.L. Trung, Homogenization approach to the behavior of suspensions of  
612 noncolloidal particles in yield stress fluids, *Journal of Rheology*, 52 (2008) 489-506.

613 [21] F. Mahaut, X. Chateau, P. Coussot, G. Ovarlez, Yield stress and elastic modulus of suspensions of  
614 noncolloidal particles in yield stress fluids, *Journal of Rheology*, 52 (2008) 287-313.

615 [22] L. Martinie, P. Rossi, N. Roussel, Rheology of fiber reinforced cementitious materials: classification  
616 and prediction, *Cement and Concrete Research*, 40 (2010) 226-234.

617 [23] H. Hafid, G. Ovarlez, F. Toussaint, P. Jezequel, N. Roussel, Effect of particle morphological  
618 parameters on sand grains packing properties and rheology of model mortars, *Cement and Concrete*  
619 *Research*, 80 (2016) 44-51.

620 [24] N. Roussel, P. Coussot, "Fifty-cent rheometer" for yield stress measurements: from slump to  
621 spreading flow, *Journal of rheology*, 49 (2005) 705-718.

622 [25] N. Roussel, C. Stefani, R. Leroy, From mini-cone test to Abrams cone test: measurement of  
623 cement-based materials yield stress using slump tests, *Cement and Concrete Research*, 35 (2005)  
624 817-822.

625 [26] N. Roussel, The LCPC BOX: a cheap and simple technique for yield stress measurements of SCC,  
626 *Materials and structures*, 40 (2007) 889-896.

627 [27] T. Nguyen, N. Roussel, P. Coussot, Correlation between L-box test and rheological parameters of a  
628 homogeneous yield stress fluid, *Cement and Concrete Research*, 36 (2006) 1789-1796.

629 [28] A. ACI, 117-Standard Specifications for Tolerances for Concrete Construction and Materials,  
630 American Concrete Institute International, (2006).

631 [29] E.I.E. de Hormigón Estructural, EHE-08 (Spanish Code Structural Concrete), Ministerio de Fomento,  
632 Madrid, (2008).

633 [30] D. Bonen, Y. Deshpande, J. Olek, L. Shen, L. Struble, D. Lange, K. Khayat, Robustness of  
634 self-consolidating concrete, in: *Proceedings of the Fifth International RILEM Symposium on*  
635 *Self-Compacting Concrete*, 2007, pp. 33-42.

636 [31] J. Rigueira, E. Taengua, P. Serna, 13. Robustness of SCC dosages and its implications on large-scale  
637 production, in: *5th International RILEM Symposium on Self-Compacting Concrete*, RILEM



638 Publications SARL, 2007, pp. 95-101.

639 [32] L. Lohaus, P. Ramge, H. Höveling, S. Anders, 12. Superplasticizer-based approach for optimized  
640 paste-composition and robustness of SCC, in: 5th International RILEM Symposium on  
641 Self-Compacting Concrete, RILEM Publications SARL, 2007, pp. 89-94.

642 [33] S. Nunes, H. Figueiras, P.M. Oliveira, J.S. Coutinho, J. Figueiras, A methodology to assess  
643 robustness of SCC mixtures, *Cement and Concrete Research*, 36 (2006) 2115-2122.

644 [34] N. Roussel, A theoretical frame to study stability of fresh concrete, *Materials and structures*, 39  
645 (2006) 81-91.

646 [35] K.H. Khayat, G. De Schutter, Mechanical properties of self-compacting concrete, state-of-the-art  
647 report of the RILEM technical committee, (2016).

648 [36] H. Bessaies-Bey, R. Baumann, M. Schmitz, M. Radler, N. Roussel, Organic admixtures and cement  
649 particles: Competitive adsorption and its macroscopic rheological consequences, *Cement and*  
650 *Concrete Research*, 80 (2016) 1-9.

651 [37] H.B. Bey, J. Hot, R. Baumann, N. Roussel, Consequences of competitive adsorption between  
652 polymers on the rheological behaviour of cement pastes, *Cement and Concrete Composites*, 54 (2014)  
653 17-20.

654 [38] P. Billberg, K.H. Khayat, Use of viscosity-modifying admixtures to enhance robustness of SCC, in:  
655 *The Third North American Conference on the Design and Use of Self-Consolidating Concrete*, 2008.

656

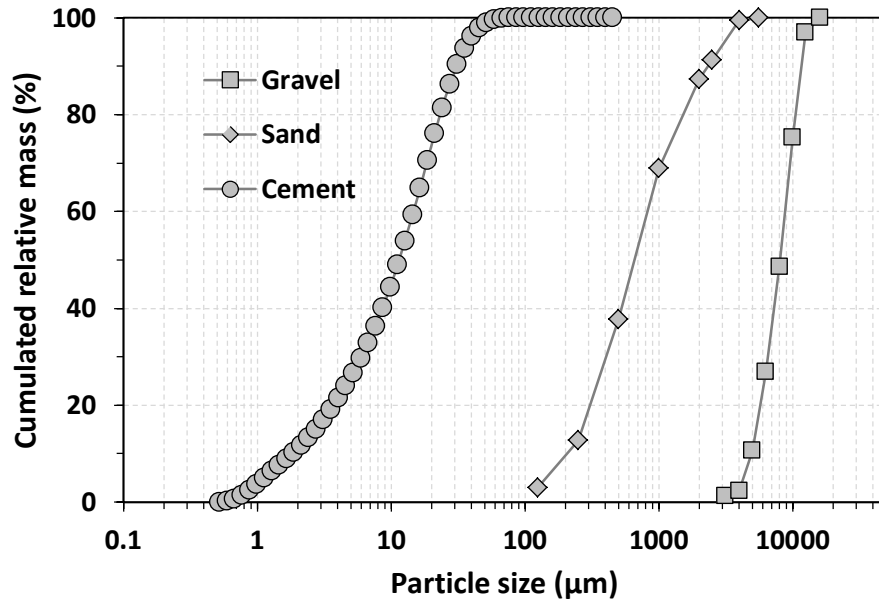


**Figure 1.** Particle size distribution of the cement and sand used in this study.

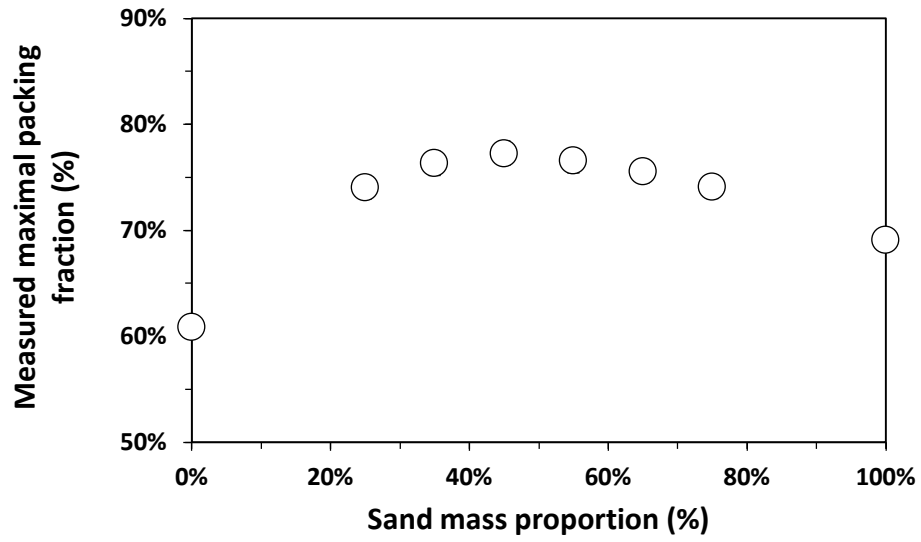


**Figure 2.** Maximal packing fraction of aggregate mixtures as a function of sand mass proportion at the level of the granular skeleton.

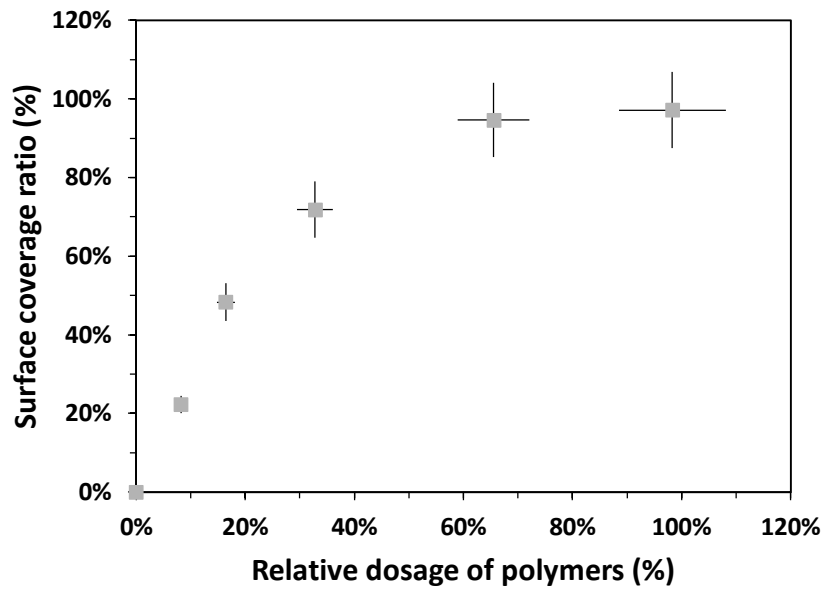


**Figure 3.** Surface coverage ratio (i.e. ratio between adsorbed polymer and adsorbed polymer at saturation) as a function of  $D_{rsp}$ , the polymer relative dosage (i.e. ratio between dosage and saturation dosage).

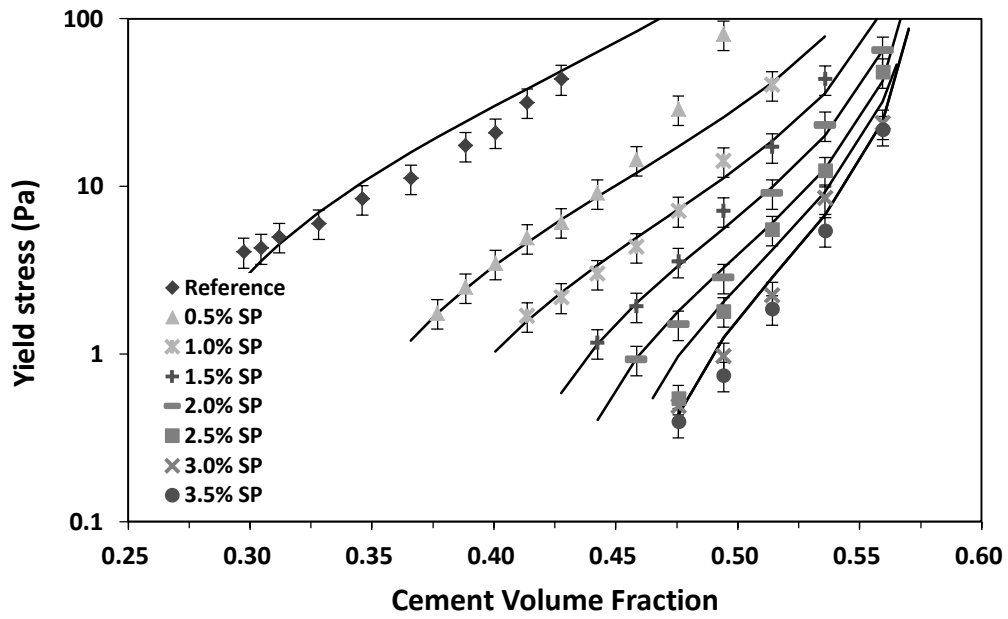


**Figure 4.** Yield stress of cement paste as a function of cement volume fraction for various SP dosages for the two types of the cement. The solid lines are the computed predictions of the YODEL.

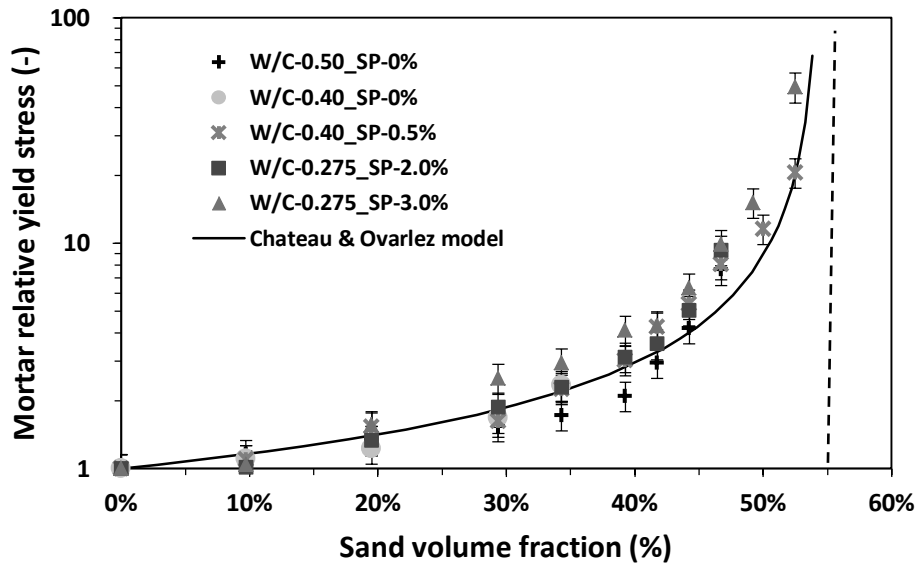


**Figure 5.** Mortar relative yield stress (i.e. ratio between the mortar yield stress and the constitutive cement paste yield stress) as a function of the sand volume fraction. The dotted vertical line corresponds to the theoretical divergence volume fraction (see text).

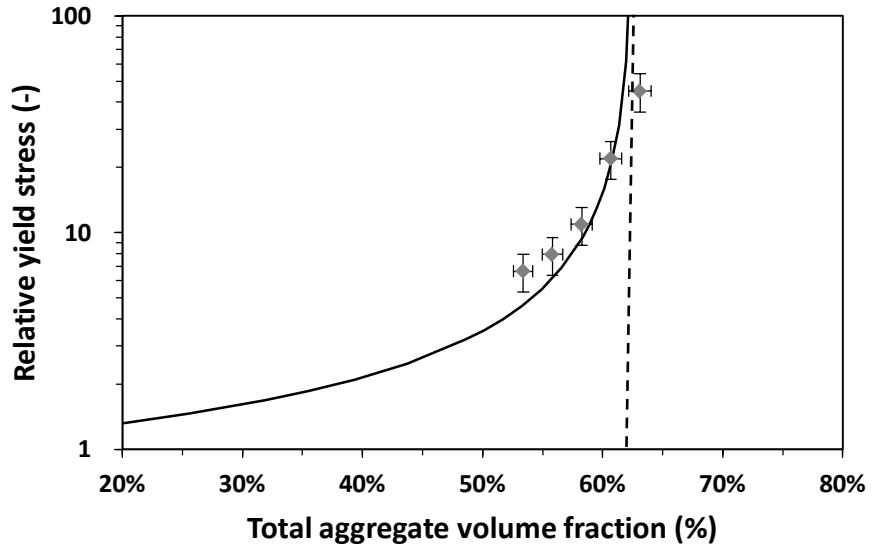


**Figure 6.** Relative yield stress of concrete as a function of aggregate volume fraction. Continuous line corresponds to the fitting of the Chateau and Ovarlez model (see text).

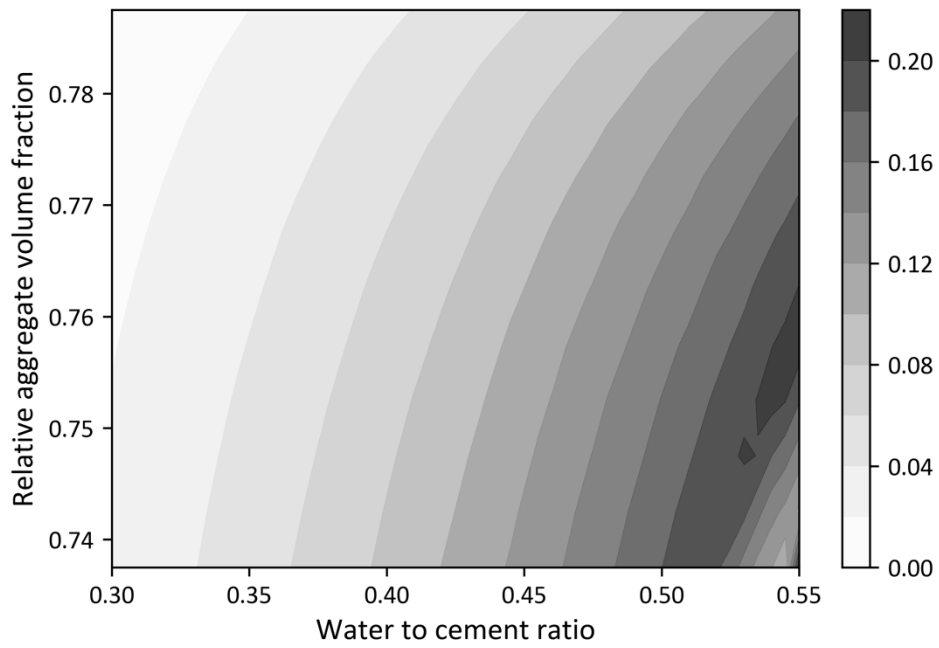


**Figure 7.** Robustness index as a function of W/C ratio and relative aggregates volume fraction for standard SP variations in industrial production. SP saturation dosage taken as 2% of the cement mass.



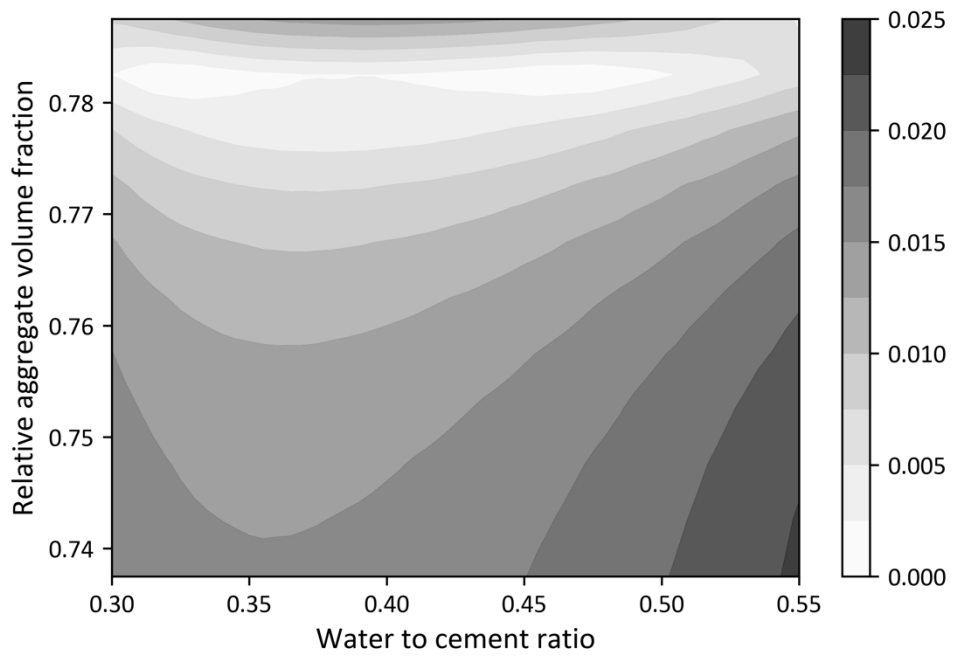


**Figure 8.** Robustness index as a function of W/C ratio and relative aggregates volume fraction for standard cement variations in industrial production.

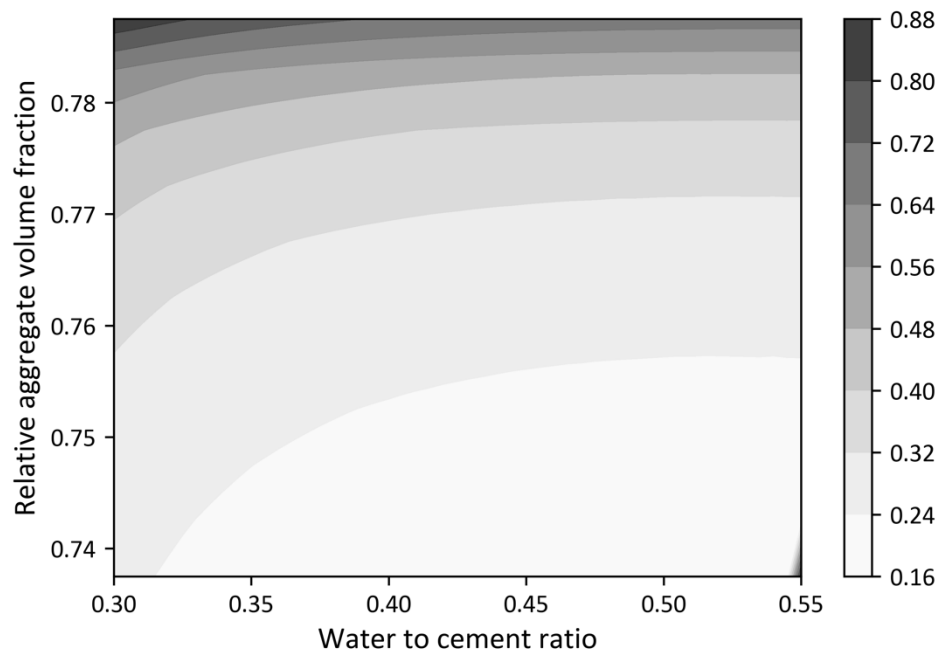


**Figure 9.** Robustness index as a function of W/C ratio and relative aggregates volume fraction for standard water dosage variations in industrial production.

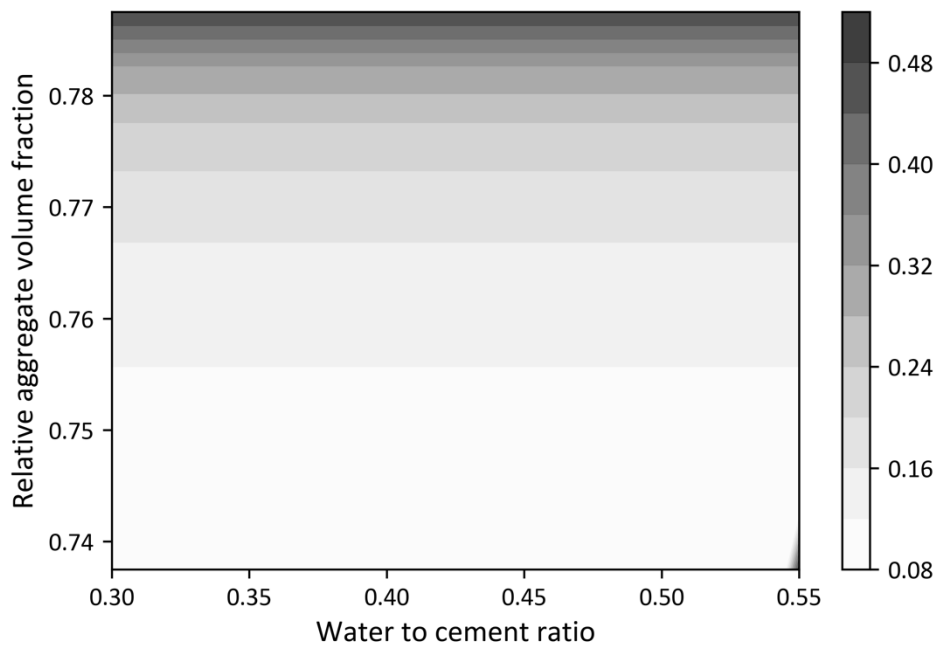


**Figure 10.** Robustness index as a function of W/C ratio and relative aggregates volume fraction for standard aggregates dosage variations in industrial production.

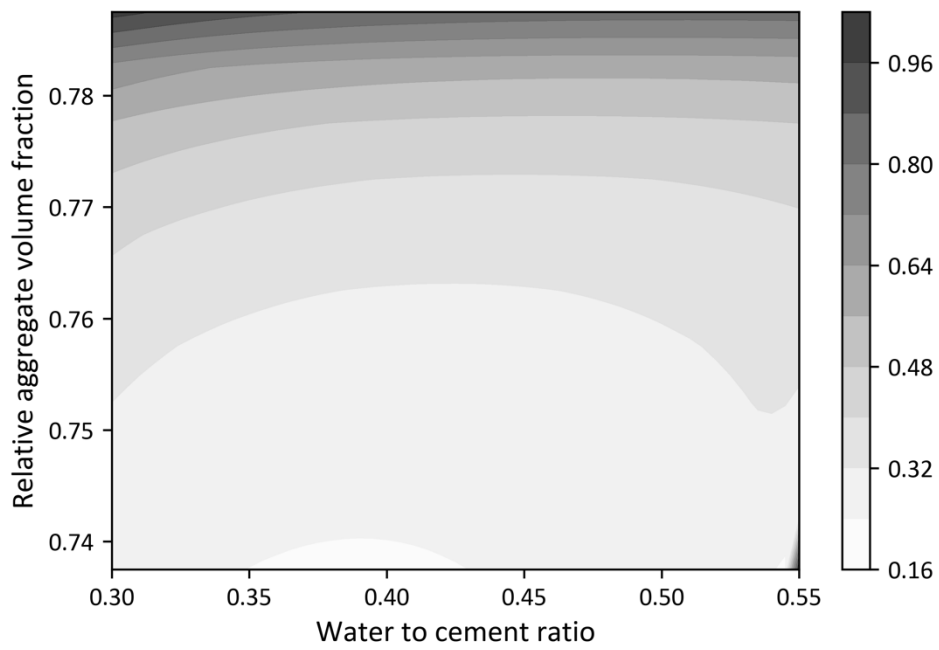


**Figure 11.** Overall robustness index as a function of W/C ratio and relative aggregates volume fraction for standard dosage variations in industrial production.

**Table 1** Chemical composition of the cement.

Composition	%Weight
SiO <sub>2</sub>	21.81%
Al <sub>2</sub> O <sub>3</sub>	3.67%
Fe <sub>2</sub> O <sub>3</sub>	5.54%
CaO	64.10%
MgO	1.31%
SO <sub>3</sub>	2.41%
Cl	0.04%

**Table 2** Aggregates properties.

Aggregates	Origin	Size range/mm	Specific density	Water absorption ratio/%	Maximum packing fraction/%
Sand	Palvadeau	0 – 4	2.64	0.6±0.05	68.3
Gravel	Seine	4 – 12	2.56	< 0.5	60.9

**Table 3** Minimum required dispenser accuracy for concrete components in a ready-mix concrete plant from existing standards.

Components	ACI limits [28]	EHE limits [29]	Absolute variation (kg/m <sup>3</sup> )
Cement	1.0%	3.0%	3
Sand	2.0%	3.0%	16
Gravel	2.0%	3.0%	24
Total aggregate content	-	-	29
Water	3.0%	3.0%	6
Admixture	3.0%	5.0%	0.15